ELSEVIER

Journal of Nuclear Materials 307–311 (2002) 778–782

journal of nuclear materials

www.elsevier.com/locate/jnucmat

Microstructure and mechanical properties of two ODS ferritic/martensitic steels

R. Schaeublin *, T. Leguey, P. Spätig, N. Baluc, M. Victoria

CRPP-EPFL, Fusion Technology Materials, 5232 Villigen PSI, Switzerland

Abstract

A microstructural analysis and tensile tests were performed on two oxide dispersion strengthened ferritic/martensitic steels. Dispersion hardening represents an interesting approach to improve the mechanical properties at elevated temperatures, as they are foreseen in the future fusion reactor, while maintaining the inherent advantages of the ferritic/martensitic steel in an irradiation environment (high thermal conductivity and low swelling rate). The base material is the ferritic/martensitic steel EUROFER 97 with the chemical composition Fe, 8.9 wt% Cr, 1.1 wt% W, 0.47 wt% Mn, 0.2 wt% V, 0.14 wt% Ta and 0.11 wt% C. In one steel the strengthening material Y_2O_3 represents 0.3 wt% while in the second it represents 0.5 wt%. It appears that the ODS with 0.3 wt% yttria presents, in terms of critical stress and uniform elongation, a better mechanical behaviour than the base material up to 500 °C and still maintains fair properties up to 700 °C.

1. Introduction

Low activation ferritic/martensitic steels are promising structural materials for the first wall of future fusion reactors that will suffer irradiation damage from the 14 MeV fusion neutrons. They have proven to be a good alternative to austenitic steels for their higher swelling resistance, about 1 vol.% per 100 dpa [1] as compared to about 1 vol.% per 10 dpa, and their lower accumulation of damage [2]. To reduce the degradation of their mechanical properties with temperature, which makes them less interesting than austenitic steels, it was proposed to strengthen these materials by a dispersion of fine oxide particles. These remain stable at temperatures up to the melting point of the base material and tend to improve the oxidation resistance of the alloy [3,4]. The strengthening results firstly from the oxide particles and secondly from the interlocked fine ferrite grain structure which results from the mechanical alloying process necessary to produce the intimate mixture between the base metal and the reinforcing particles. These fine ferrite grains present Cr carbide decoration at their boundaries and form a bamboo structure, which comes from the hot extrusion process after the mechanical alloying. Both are detrimental to mechanical properties, and recrystallisation routes are designed to produce more equiaxed grains [5]. A number of studies has shown that the mechanical properties of given ferritic/martensitic steels are indeed improved by the oxide dispersion and that they retain a better behaviour at high temperatures, between 600 and 900 °C [6,7]. The ductile-to-brittle transition temperature was, however, shown to be increased by the addition of the oxide dispersion in a 13% Cr ferritic steel [8]. It should be noted also that the segregation behaviour induced by heat treatments can be modified by the oxide dispersion. A pronounced Cr segregation to the oxide particle interface was found after annealing at 700 °C in a Fe–Cr alloy [9]. Two types of oxides are generally considered, namely yttria, Y_2O_3 and titanium oxide, TiO_2. The Y_2O_3 containing alloy appears, however, to be slightly superior to the TiO_2 dispersion in a 13% Cr, 1.5% Mo and 2–3% Ti ferritic steel [10]. In addition, Ti tends to segregate to grain

* Corresponding author. Tel.: +41-56 310 40 82; fax: +41-56 310 45 29.
E-mail address: robin.schaeublin@psi.ch (R. Schaeublin).

PII: S0022-3115(02)01193-5

boundaries [11] and to promote χ phase formation at high temperatures above 800 °C [12], both being detrimental to strength and ductility. In terms of radiation resistance it was recognized that the oxide dispersion strengthened (ODS) ferritic steels are similar if not better relatively to their base material. In the yttria strengthened steels, the swelling rate is maintained to a low level, 0.5% per 100 dpa as deduced from ion irradiation in an ODS 13% Cr ferritic steel [13] and 1–2% per 100 dpa as deduced from electron irradiation [14,15]. Moreover, it appears that the microstructure of ODS ferritic steels exhibit a promising stability under irradiation. Under electron irradiation the dislocation microstructure and the yttria particles in a 13% Cr alloy remain almost constant after 12 dpa [16]. After 30 dpa, it was found that yttria particles are still unchanged [17]. In addition, no voids were identified, while they were present for the same conditions in the irradiated base material [17].

A European ODS steel is being developed on the base of the EUROFER 97 ferritic/martensitic steel with yttria particles for strengthening. The mechanical properties and the microsctructure of two grades of this ODS steel are examined. We show that the reinforced EUROFER 97 containing 0.3% yttria has a better mechanical behaviour in tension up to 500 °C and fair up to 700 °C relatively to the base material.

2. Experimental

The investigated ODS steels are based on the ferritic/martensitic steel EUROFER 97 (150 μm powder grain size) that has a composition of about 8.9% Cr, 1.1% W, 0.47% Mn, 0.2% V, 0.14% Ta and 0.11% C and Fe for the balance. The strengthening particles are composed of yttria, Y_2O_3, and the material was prepared by hot isostatic pressing (HIP) at Plansee, Austria. Two cases are studied, one where yttria represents 0.3% and the other 0.5%.

Transmission electron microscopy (TEM) samples were punched out from thin 0.3 mm plates. TEM was performed at 200 kV on a JEOL2010 using conventional bright field/dark field imaging. Energy dispersive X-ray spectrometry (EDS) was used to distinguish the oxide particles from the carbides with an Oxford Si(Li) detector. The oxide particle size distribution was determined from dark field images that were processed before the size distribution measurement [18]. The image background was removed and the resulting image was binarized by selecting a grey level threshold that allows to delineate the yttria particles as closely as possible.

Specimens were cut by electroerosion as flat tensile test specimens (0.3 mm thickness, 2.5 mm width and 8 mm gauge length) that are suitable for irradiation in the PIREX (Proton IRradiation EXperiment) facility. Tensile deformation experiments were conducted up to failure in an argon flow in a Zwick uniaxial testing machine, from room temperature to 700 °C with a strain rate of 4×10^{-5} s^{-1}. A comparison with DIN 3 mm cylindrical specimens deformed on a Schenck RMC100 machine validated the PIREX sample geometry.

3. Results

The microstructure of both as-received ODS steels is presented in Fig. 1. In the scanning electron microscope the surface appears smooth in the case of the 0.3% yttria, while the 0.5% yttria reveals pores that are about 10 μm in size. In TEM, both ODS steels present interlocked ferrite grains, the boundaries of which are decorated with Cr carbides of the $Cr_{23}C_6$ type (Fig. 1(a) and (b)). In the case of the 0.5% yttria, the carbides at the grain boundaries with sizes up to about 1 μm are larger than in the case of the 0.3% yttria, where they attain about 0.2 μm maximum. The grain size of about 5 μm in both ODS steels is smaller than in the case of the base tempered martensite EUROFER 97, which presents grains of about 15 μm in size that are decomposed in a martensite lath structure. Note that no clear microstructural difference could be identified between the transverse and the longitudinal cuts, as for the tensile test response. Fig. 1(c) and (d) reveal the yttria particles. They appear heterogeneously distributed, with regions free of them. This is examplified in Fig. 1(c) for 0.3% yttria, where only the bottom left quadrant exhibits yttria. This is also apparent for 0.5% yttria in Fig. 1(d), where only the right part of the central grain presents yttria dispersion. Yttria particles appear in the material in either groups of about 20–40 nm round particles or groups of 1–5 nm round particles. Rarely do the two populations mix. Yttria particles follow a normal skewed gaussian distribution with a mean size of 3.8 nm. Note that the 20–40 nm yttria particle distribution resembles nearly parallel bead strings (Fig. 1(c) and (d)).

Mechanical testing results as a function of temperature are summarized in Table 1. The case of the 0.3% yttria presents, relatively to EUROFER 97 and up to 500 °C, an increase of the critical stress measured at 0.2% plastic strain of more than 100 MPa and increase of the ultimate tensile strength (UTS) of more than 200 MPa. Above 500 °C, the differences diminish and at 600 °C only the UTS favours the ODS steel over the base material. The uniform elongation of the ODS 0.3% is higher over the whole temperature range, while at low temperatures the elongation at failure of the base material is shorter but then strongly increases above 450 °C and overcomes the one of the ODS steel. Note that values for EUROFER 97 at 500 and 600 °C are taken from [19]. The case of the 0.5% yttria is not so promising, with a critical stress similar or lower than the one of the base material, and similar or lower elongations.

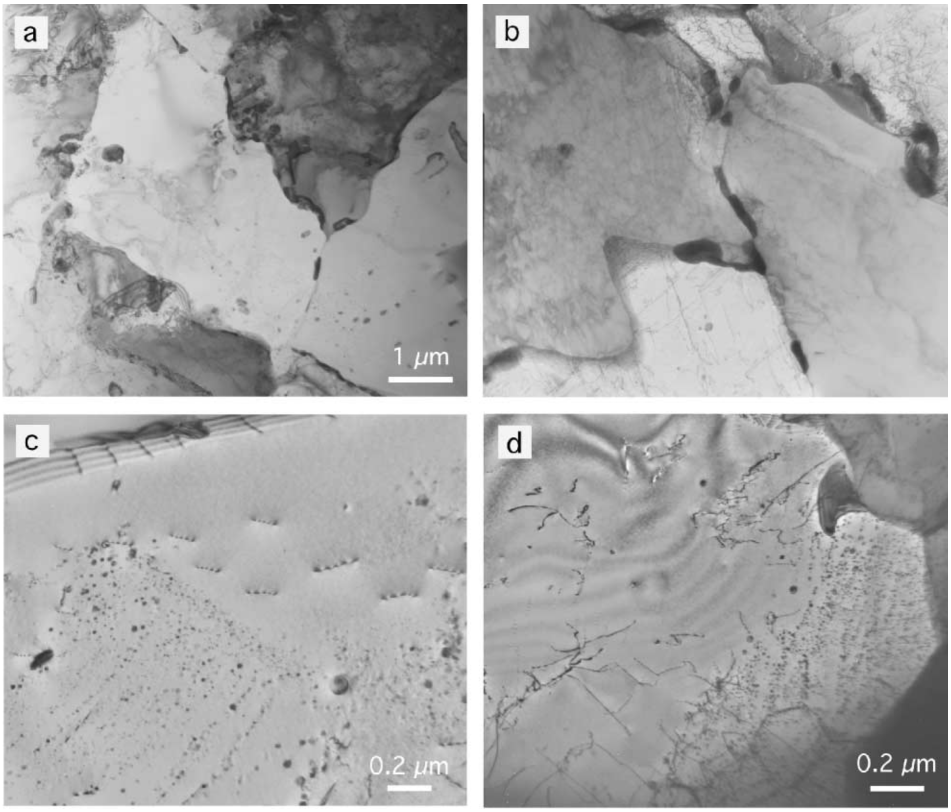

Fig. 1. TEM micrographs showing the interlocked ferrite grains decorated at the grain boundaries with carbides in (a) 0.3 wt% and (b) 0.5 wt% yttria, and showing the yttria particle distribution in (c) 0.3 wt% and (d) 0.5 wt% yttria.

Table 1
Critical tensile strength, $\sigma_{0.2}$, ultimate tensile strength, σ_u, uniform elongation, ε_u and elongation at failure, ε_f, of the ODS EUROFER 97 with 0.3 and 0.5 wt% yttria and of EUROFER 97

T (°C)	ODS 0.3% yttria				ODS 0.5% yttria				EUROFER 97			
	$\sigma_{0.2}$ (MPa)	σ_u (MPa)	ε_u (%)	ε_f (%)	$\sigma_{0.2}$ (MPa)	σ_u (MPa)	ε_u (%)	ε_f (%)	$\sigma_{0.2}$ (MPa)	σ_u (MPa)	ε_u (%)	ε_f (%)
20	698	915	9.7	14.8	633	745	3	3.3	565	655	4.8	14.8
150									532	600	3.4	13
200	643	832	13.5	17.2	456	640	4.1	4.2				
250									485	564	3.1	12.7
300	671	821	12.8	13.9	472	594	2.8	2.8				
350									480	528	2.2	11.1
400	600	800	10.6	14.5	454	570	3.3	3.4				
450									440	490	2.2	11.2
500	516	694	4.9	10.5	344	464	2.9	3	400[a]	440[a]	2[a]	23[a]
600	326	415	4	10.7	242	296	4.3	4.6	300[a]	320[a]	1.5[a]	33[a]
700	210	272	5.1	9.3	146	146	2	2.3				

[a] From [19].

SEM observations of the fracture faces displayed in Fig. 2 show that there is visible reduction of area in the case of the 0.3% yttria at 700 °C (Fig. 2(a)) and at room temperature (Fig. 2(b)). In the case of the 0.5% yttria there is no visible necking at both temperatures (Fig. 2(c) and (d)), while porosity and individual grains can be distinguished. At higher magnification there is indication for localized ductility in both materials at both

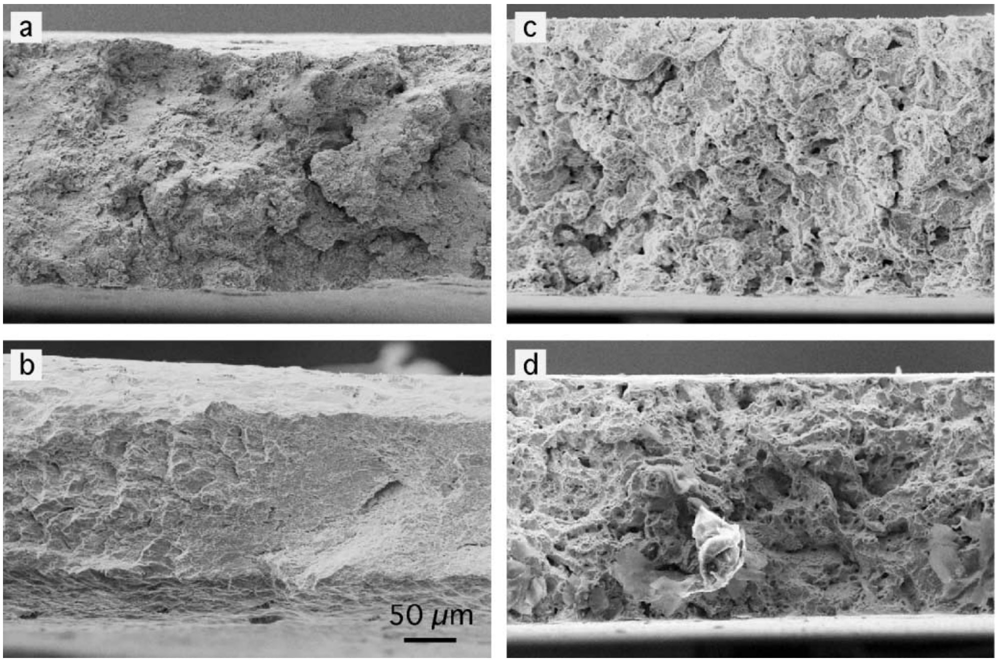

Fig. 2. SEM micrographs of the fracture face of ODS steel with 0.3 wt% yttria at (a) 700 °C and (b) room temperature and with 0.5 wt% yttria at (c) 700 °C and (d) room temperature.

temperatures. The general fracture mode, however, seems to be intergranular in nature.

In summary, while the case of the 0.3% yttria containing EUROFER 97 steel has superior tensile resistance and similar, if not better, uniform elongation behaviour than the base material, the case of the 0.5% yttria presents weak mechanical properties. It presents a microstructure that cannot sustain stresses even to the level of the base material. This fact is certainly related to the presence of the porosity observed in SEM and to the large carbides observed in TEM. The heat treatment should be responsible for this situation, as the yttria dispersion presents the same size and spatial distributions as the ones found in the case of the 0.5% yttria. The porosity indicates that the HIP process has to be improved. The Concentration of yttria seems also to be of importance for the mechanical properties of the ODS alloy.

4. Conclusions

The EUROFER 97 reinforced with 0.3% yttria presents better tensile properties than the base material. At room temperature it shows a critical stress of more than 900 MPa, which corresponds to an increase of 200 MPa and a uniform elongation that is double relatively to the base material. At 700 °C the yield stress is still 210 MPa. The uniform elongation at room temperature of about 10% is, when compared to the 5% of the base material, reasonable for a ferritic steel. At 700 °C, this elongation is still of about 5%.

Acknowledgements

M. Grosse, PSI, is gratefully acknowledged for collaboration with SEM and The Paul Scherrer Institut is thanked for overall use of the facilities.

References

[1] D.S. Gelles, J. Nucl. Mater. 233–237 (1996) 293.
[2] R. Schäublin, D.S. Gelles, M. Victoria, these Proceedings.
[3] G.M. McColvin, G.D. Smith, International Conference on High Temperature Alloys: Their Exploitable Potential. Comm. Eur. Communities, Luxembourg, 1985, p. 12.
[4] H. Cama, T.A. Hughes, Electron Microscopy and Analysis 1993, in: Proceedings of the Institute of Physics Electron and Analysis Group Conference, IOP Publishing, Bristol, UK 1993, p. 361.
[5] S. Ukai, T. Nishida, H. Okada, T. Okuda, M. Fujiwara, K. Asabe, J. Nucl. Sci. Technol. 34 (1997) 256.
[6] D.K. Mukhopadhyay, F.H. Froes, D.S. Gelles, J. Nucl. Mater. 258–263 (1998) 1209.
[7] G.R. Romanoski, L.L. Snead, R.L. Klueh, D.T. Hoelzer, J. Nucl. Mater. 283–287 (2000) 642.

[8] J. Sun, C. Chen, X. Zhang, Y. Tian, B. Shan, Q. Pan, Acta Metall. Sin. 34 (1998) 1210.
[9] A.V. Krajnikov, H.M. Ortner, S. Weinbruch, W. Grogger, P. Warbichler, F. Hofer, V.M. Yurchenko, Mater. Sci. Technol. 15 (1999) 1425.
[10] J.J. Huet, Sintered Metal-Ceramic Composites, in: Proceedings of the Third International School on Sintered Materials, Elsevier, Amsterdam, The Netherlands 1984, p. 197.
[11] M.A. Miodownik, J.W. Martin, E.A. Little, J. Mater. Sci. Lett. 12 (1993) 834.
[12] Y. Tian, Q. Pan, G. Liu, B. Shan, F. Yang, Acta Metall. Sin. 34 (1998) 1217.
[13] E.A. Little, D.J. Mazey, W. Hanks, Scripta Metall. Mater. 25 (1991) 1115.
[14] F. Wan, X. Huang, F. Kong, W. Chu, J. Xiao, H. Takahashi, Acta Metall. Sin. 30 (1994) 448.
[15] B. Hu, C. Wu, T. Hesishichiro, Acta Metall. Sin. 31 (1995) 525.
[16] J. Saito, T. Suda, S. Yamashita, S. Ohnuki, H. Takahashi, N. Akasaka, M. Nishida, S. Ukai, J. Nucl. Mater. 258–263 (1998) 1264.
[17] H. Kinoshita, N. Akasaka, H. Takahashi, M. Itoh, S. Onose, J. Nucl. Mater. 179–181 (1991) 722.
[18] J.C. Russ, The Image Processing Handbook, 3rd Ed., CRC, 1998.
[19] H.E. Hofmans, Tensile and impact properties of EUROFER 97 plate and bar, NRG report 20023/00.38153/P, Petten, The Netherlands, 2000.